Journal of Marine Science and Technology, Vol. 21, No. 1, pp. 51-57 (2013)
DOI: 10.6119/JMST-011-0831-1

EXPERIMENTAL STUDY OF THE REVERSE CONVERSION OF WAVE SPECTRA

Beng Chun Lee[1], Yang-Ming Fan[2], Xiangbo Feng[3], and Chia Chuen Kao[4]

Key words: wave spectrum transform coefficient, peak energy, wave tank experiment.

ABSTRACT

The observed deep-sea wave data are most appropriate to use in the data assimilation technique. For wave stations (e.g., the Longdong data buoy station in the northeastern Taiwan Sea near the coast), wave data must be reverse-calculate deep-sea wave data for data assimilation applications because seafloor slopes in the northeastern Taiwan Sea are acute and the distances between wave interactions during propagation are shorter. Consequently, nonlinear effects arising from the topography become insignificant as waves approach the coast from the open sea. The proposed technique to reverse-calculate the deep-sea wave spectrum from the near-shore wave spectrum, based on first-order wave spectrum theory, is verified based on physical experiments. The results indicate that this method is effective and applicable to calculations of the energy at wave spectrum peaks.

I. INTRODUCTION

The application of data assimilation techniques in wave forecasts has been hampered due to a lack of high-quality wave data measurements. Recently, data assimilation techniques have gradually been incorporated into numerical wave models due to rapid developments in satellite observation technology and an increase in the number of on-site monitoring wave stations. Currently, 11 operational wave stations immediately transmit hourly wave data via wireless communication from sea sites to onshore stations in Taiwan's marine regions. These data provide an excellent basis for testing data assimilation techniques.

Near-shore data buoys are located around the coast of Taiwan. Data assimilation techniques in numerical wave models are best suited to deep-sea wave data because the purpose of data assimilation is to make imminent wave forecasts. By the time that near-shore data have been substituted into the data assimilation process and further into the wave models, the waves will have already reached the shores. In this situation, wave forecasts are useless. Therefore, it is essential that deep-sea wave data be assimilated.

Because deep-sea wave data are unavailable for use in the data assimilation process, this paper proposes a method that deduces the deep-sea region wave spectrum based on calculations of the near-shore wave spectrum. This method differs from the general wave spectrum calculations that evaluate waves originating in the deep-sea region that propagate toward the shore [2, 6, 7]. Instead, this method reverse-calculates the wave spectrum from near the shore to the deep sea. If nonlinear effects are accounted for in calculating wave shoaling, the calculations become very complex. Previously, Chien and Kuo [1] performed a thorough study of the nonlinearity of the shallow-water wave spectrum and found that the spectrum is linear most of the time. In addition, based on results from Kuo *et al*. [4], who used wave tank experiments to study the propagation of irregular waves in one direction, the non-dimensional wave spectral shape is similar to that of the deep-water wave spectrum as long as the water depth is constant in the shallow water region. However, as the water depth is reduced, the wave spectrum shape attenuates more slowly.

In this paper, the northern tip of Taiwan is used as a case study to investigate the proposed method. Because the slope of the sea bottom in this area is steep, the distances between the wave interactions during propagation are short, and nonlinear effects are not significant. Thus, it is appropriate to use linear wave calculations to deduce the deep-sea wave spectra from coastal wave data. However, because the wave stations used in this study do not collect measurements in shallow water, even when the waves do not break, the nonlinear contribution due to the nonlinear wave-wave interaction term S_{nl} in the source term of the numerical wave model can be neglected. In addition, wind input and white

Paper submitted 07/23/10; revised 03/04/11; accepted 08/31/11. Author for correspondence: Beng Chun Lee (e-mail: beng@huafan.hfu.edu.tw).
[1] *Department of Environmental and Hazards-Resistant Design, Huafan University, New Taipei City, Taiwan.*
[2] *Coastal Ocean Monitoring Center, National Cheng Kung University, Tainan City, Taiwan.*
[3] *College of Harbor, Coastal and Offshore Engineering, HoHai University, Nanjing, P.R.China.*
[4] *Department of Hydraulics & Ocean Engineering, National Cheng Kung University, Tainan City, Taiwan.*

capping dissipation are assumed to be small at short distances.

II. REVERSE CONVERSION OF THE WAVE SPECTRUM

The wave spectrum is the superposition of many waves of differing energies (magnitudes and frequencies) if the near-shore wave spectrum density function is known, the integrated frequency domain of the wave energy density function is:

$$E = \int_0^\infty S(f)df = \sum_{i=1}^{\infty} S(f_i)\Delta f_i = \sum_{i=1}^{\infty} E_{f_i} \tag{1}$$

where Δf_i is the corresponding frequency width of any arbitrary frequency, f_i, and the energy of each specific frequency width is:

$$E_{f_i} = S(f_i)\Delta f_i \tag{2}$$

According to the small amplitude wave theory, waves are assumed to be tangential to shores, and the seafloor is assumed to be of uniformly slope. Three wave energy components, breaking waves, leak from the sea bottom, and frictional energy loss of the waves, are disregarded under the stationary wave fields. The wave energy fluxes before and after wave shoaling are then equal. Therefore, the wave energy flux conservation equation of f_i can be written as follows:

$$\left(E_{f_i} c_{f_i} n_{f_i}\right)_o = \left(E_{f_i} c_{f_i} n_{f_i}\right)_d \tag{3}$$

where $n = \frac{1}{2}(1 + \frac{2kd}{\sinh kd})$, $n = \frac{1}{2}$ in deep water, o indicates the deep-water physical quantity, d the shallow-water physical quantity, and c the phase speed.

Substituting Eq. (2) into Eq. (3) yields:

$$\left(S(f_i)\Delta f_i c_{f_i} n_{f_i}\right)_d = \left(S(f_i)\Delta f_i c_{f_i} n_{f_i}\right)_o \tag{4}$$

Because each specific frequency width remains uniform before and after wave shoaling, Eq. (4) can be simplified as:

$$\frac{\left(S(f_i)\right)_o}{\left(S(f_i)\right)_d} = \frac{\left(c_{f_i} n_{f_i}\right)_d}{\left(c_{f_i} n_{f_i}\right)_o} \tag{5}$$

If $(S(f_i))_o/(S(f_i))_d$ is equivalent to $K_{spectrum}(f_i)$, the deep-water wave spectrum transform coefficient, the wave spectral density variation of the frequency f_i is written as:

$$K_{spectrum}(f_i) = \frac{\left(c_{f_i} n_{f_i}\right)_d}{\left(c_{f_i} n_{f_i}\right)_o} \tag{6}$$

$$(2\pi)^2 \cdot f_i^2 = g k_{f_i} \tanh(k_{f_i} d) \tag{7}$$

Based on the dispersion relationship described in Eq. (7), the formula of the transform coefficient can be obtained from Eq. (8) as:

$$K_{spectrum}(f_i) = (1 + \frac{2k_{f_i} d}{\sinh 2k_{f_i} d}) \tanh k_{f_i} d \tag{8}$$

Because f_i is an arbitrary selected frequency, Eq. (8) is also applicable to calculate the deep-water wave spectrum transform coefficients for all frequencies. Thus, the transform coefficient of the deep-water waves can be obtained from Eq. (8) by reverse calculation of the near-shore-wave-spectrum. If the near-shore wave spectrum is known, then the linear calculation of the deep-water wave spectrum is simply the first-order wave spectrum:

$$S'(f_i) = K_{spectrum}(f_i) S(f_i) \tag{9}$$

III. EXPERIMENT TESTS

Although we cannot obtain the deep-water wave data, the first-order deep-water spectra can be determined based on the reverse conversion of the wave spectrum derived in this study. The basic assumption of this method is that the wave effect of nonlinearity is insignificant when the seafloor is steep. The use of wave tank experiments that demonstrate the effect of physical wave phenomena is the only viable method that can reproduce the actual setting and verify the applicability of this method. Furthermore, field data cannot be collected on-site; however, these data can be obtained in the wave tank experiments.

1. Scale Setting in the Wave Tank Experiments

The simulation of long-period waves around the north-eastern tip of Taiwan is the first step in determining the initial conditions for the data assimilation process. The Longdong data buoy is located off the coast of the Long Dong yacht harbor. The buoy is positioned approximately 2 km offshore, where the water is approximately 30 m deep (Fig. 1). The wave data observed at this inshore station can be used as a basis for calculating deep-water spectra. As shown in Fig. 1, the location of the Longdong data buoy slopes more in the direction of the open water, so the distances between wave interactions during propagation are short. Based on this characteristic, it can be assumed that the nonlinear effects are not significant and that it is appropriate to adopt the linear wave theory developed in this study.

Therefore, based on the selected sea area, a proportional area size can be used for the wave tank experiments. The scale settings are shown in Table 1; the wave tank capacity and local environment were reduced 150-fold in space and

Table 1. Comparison of bit error rates for the simulation.

	On-site	Experiment	Space scale	Time scale
Near-shore sea depth (m)	30	0.2	150:1	$\sqrt{150}$:1
Off-shore sea depth (m)	80	0.8 > 0.53 (dmin)*		
Significant wave length (m)	15	0.1		
Significant wave height (m)	160	1.1		
Significant wave period (sec)	10	0.8		

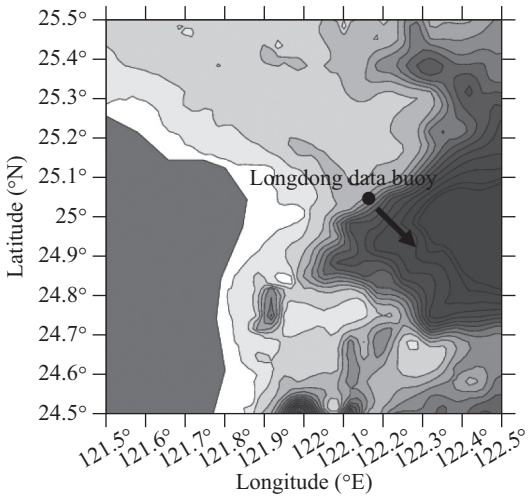

Fig. 1. Water depths in the northeastern Taiwan Sea. The Longdong data buoy location is marked. The red arrow indicates the incline of the sea floor.

12.5-fold in time. To ensure that the variations in the spectrum are caused by wave shoaling and not by wave energy dissipation due to the experimental apparatus used, this study used a regular-wave experiment to confirm that the waves were conserved after installation of the experimental apparatus. The wave spectrum experiments were then conducted to analyze the irregular waves.

2. Experiment Apparatus and Set-up

The experiments were conducted in a cross-sectional tank at the Department of Hydraulic & Ocean Engineering, Cheng Kung University, of total length 27 m, width 1 m, height 1.4 m, and water depth 0.8 m (Fig. 2). The front tip of the wave-generation panel was the benchmark bottom panel. A 1:10 slope made of stainless steel bottom board began 10 m from the wave generator. Both sides of the tank were made of transparent glass plates, and the wave generator generated regular and irregular waves. Four resistance-type wave gauges divided into 2 sets of 2 gauges each were installed within the tank. One set was installed at a depth of 0.2 m

Table 2. Conditions for regular wave experiments.

Experiment No.	Significant wave height, H_s (m)	Significant wave period, T_s (sec)
R1	0.04	1.1
R2	0.08	0.8
R3	0.09	1

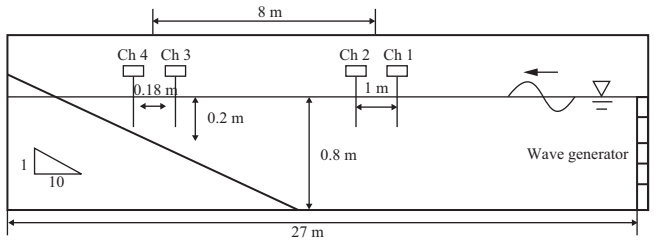

Fig. 2. Experimental tank setup.

with a wave-height gauge spacing of 0.18 m for observing shallow-water waves; the second set was established at a depth of 0.8 m from the first set with a wave-height gauge spacing of 1 m.

3. Experimental Procedure

1) Regular Wave Experiments

In the theory of deducing wave spectra shoaling, it is assumed that the wave energy flux is conserved, as shown in Eq. (3). To ascertain that the spectrum calculations are reasonable, regular wave experiments were initially conducted to verify that the wave energy flux was conserved following installation of the experimental apparatus.

The conditions to generate near-shore waves in these experiments using the wave generator are shown in Table 2. The waves that are generated are influenced by the water depth as they propagate toward the shallow-water wave height gauges. The experiments were grouped into three sets using a continuous observation time of 120 seconds, and the sample frequency was 60 Hz for each set.

2) Irregular Wave Experiments

Chien and Kuo [1] analyzed the wave spectra of Taiwan's northeastern cape and found that the spectral distribution obtained at this location was consistent with a JONSWAP spectrum [3]. The non-dimensional wave spectra obtained from the Longdong data buoy (longitude 121°56'35", latitude 25°2'11"; water depth 15 m) show that the spectral shape at this location also appears to be a JONSWAP spectrum [8].

Therefore, the JONSWAP spectrum can reasonably be taken as a basis for the irregular wave experiments conducted in this study. Ou [5] analyzed waves observed in the waters offshore of Taiwan, and the coefficients taken from their results are shown in Eq. (10), where H_s is the significant wave height and T_s is the significant wave period.

Table 3. Conditions for irregular (JONSWAP spectrum) wave experiments.

Experiment No.	Significant wave height, H_s (m)	Significant wave period, T_s (sec)
IR1	0.1	0.8
IR2	0.1	0.9
IR3	0.1	1
IR4	0.1	1.1
IR5	0.1	1.2
IR6	0.1	1.3
IR7	0.1	1.4

$$S(f)=\frac{3.28}{C_1^2C_2^4}\left(\frac{H_s}{T_s^2}\right)\cdot f^{-5}\exp\left[-1.25\left(C_2\cdot f\cdot T_s\right)^{-4}\right]\cdot\gamma^{\exp(\beta)}$$

$$\begin{cases}\beta=-\dfrac{1}{2\sigma_0^2}\left(C_2\cdot f\cdot T_s-1\right)^2\\ C_1=3.8\\ C_2=1.13\\ \gamma=2.08\\ \begin{cases}\sigma_0=0.07, & f\le f_p\\ \sigma_0=0.09, & f>f_p\end{cases}\end{cases}\tag{10}$$

Six experiments were conducted using the wave generating conditions presented in Table 3. To simplify analysis, the significant wave height was universally set to 0.1 m, and the significant wave period was set to 0.8-1.4 sec. The persistent observation time was 120 sec for every group, and the sampling frequency was 60 Hz. The wave height gauge placed in the deep-water region measures water height variations before wave shoaling; the wave height gauge on the slope measures water height variations only after wave shoaling.

4. Experimental Analysis

1) Regular Wave Experiments — Analysis of the Conservation of Wave Energy Flux

The main purpose of the regular wave experiments was to test the conservation of wave energy flux following installation of the apparatus; if the wave energy flux is conserved, this result provides evidence that the following spectral analysis is reasonable. The energy flux formula, shown in Eq. (3), calculates the phase speed for the waves. The wave phase difference for the fixed distance between the two wave height gauges was utilized in this study to obtain the phase speed (Figs. 3 and 4).

The results for the wave energy flux calculations are shown in Fig. 5, and these results are readily observed in experiments No. R2 and No. R3. A rather small error (within a relative error of 5%) exists for the wave energy flux that occurs in both the deep- and shallow-water regions. Although

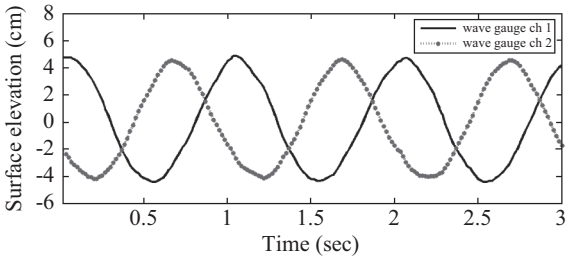

Fig. 3. The time series for the two wave gauges on both sides of the tank in the deep-water regions (distance between the wave gauges: 1 m).

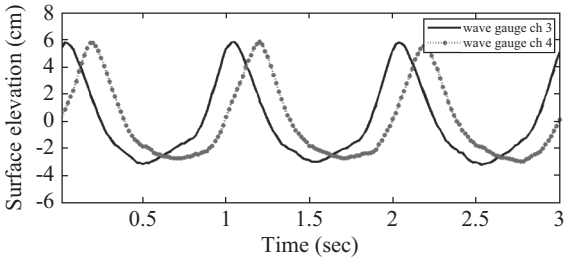

Fig. 4. The time series for the two wave gauges on both sides of the tank in the shallow-water regions (distance between the wave gauges: 0.18 m).

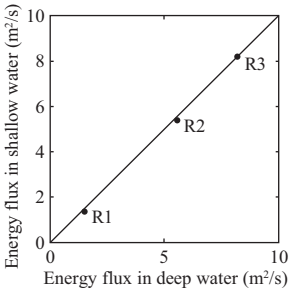

Experimen No.	Relative Error (%)
R1	10.67
R2	3.41
R3	0.00

Fig. 5. The calculated values and error analysis for the wave flux energy in the water tank.

the relative error for experiment No. R1 reaches 10.67%, this error is due to the small magnitude of the wave energy in this experiment, and the effects of the measured error are minor. Therefore, the wave energy flux is conserved during the wave propagation process within the tank, and the depletion of wave energy is not significant. Thus, the experimental apparatus satisfies the requirements of the subsequent reverse calculation experiments.

2) Irregular Wave Experiments — Analysis of the Applicability of Reverse Calculations of the Wave Spectrum

The purpose of the irregular wave experiments is to verify the applicability of the linear calculation of the wave spectrum. The analysis procedure is described below.

(a) The corresponding spectrum transform coefficient, $K_{spectrum}$, which is distributed over the frequency domain using

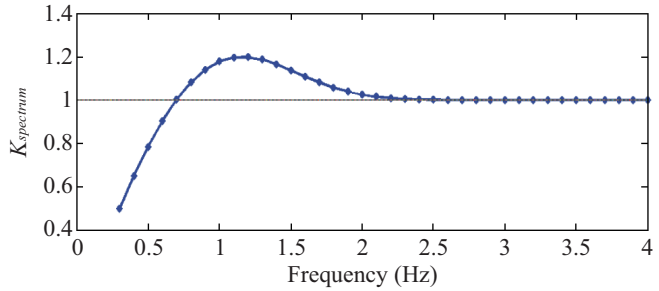

Fig. 6. The calculated distribution of the linear spectrum transform coefficients over the frequency domain (Water depth: 0.2 m; frequency resolution: 0.1 Hz).

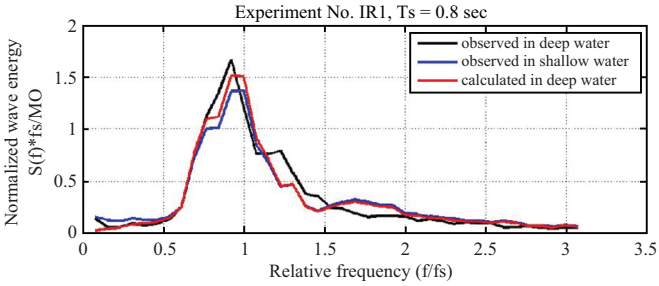

Fig. 7. A comparison of the reverse-calculated wave energy values and the experimental wave energy values (significant wave period Ts = 0.8 sec). f_s is the significant wave period in relation to the corresponding significant frequency.

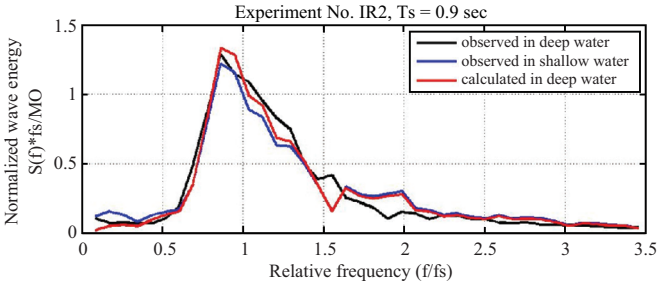

Fig. 8. A comparison of the reverse-calculated wave energy values and the experimental wave energy values (significant wave period Ts = 0.9 sec). f_s is the significant wave period in relation to the corresponding significant frequency.

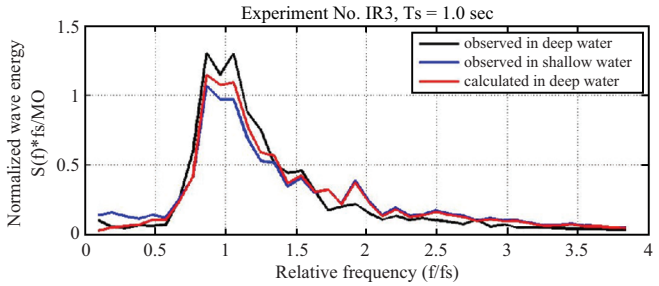

Fig. 9. A comparison of the reverse-calculated wave energy values and the experimental wave energy values (significant wave period Ts = 1.0 sec). f_s is the significant wave period in relation to the corresponding significant frequency.

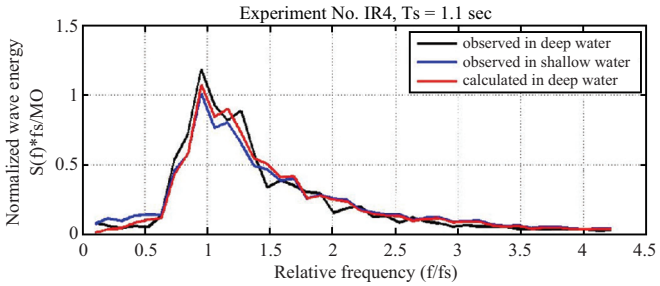

Fig. 10. A comparison of the reverse-calculated wave energy values and the experimental wave energy values (significant wave period Ts = 1.1 sec). f_s is the significant wave period in relation to the corresponding significant frequency.

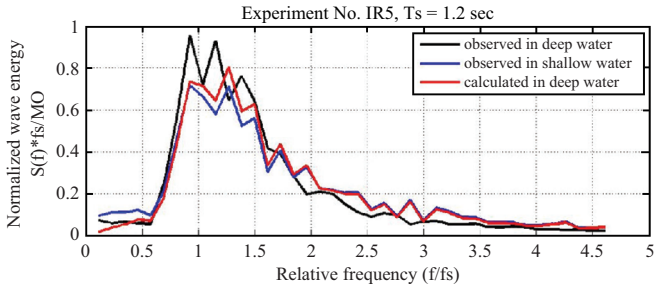

Fig. 11. A comparison of the reverse-calculated wave energy values and the experimental wave energy values (significant wave period Ts = 1.2 sec). f_s is the significant wave period in relation to the corresponding significant frequency.

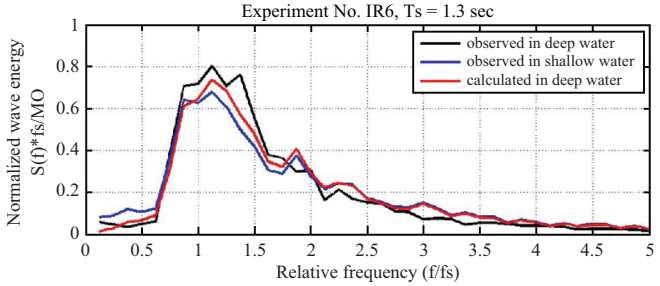

Fig. 12. A comparison of the reverse-calculated wave energy values and the experimental wave energy values (significant wave period Ts = 1.3 sec). f_s is the significant wave period in relation to the corresponding significant frequency.

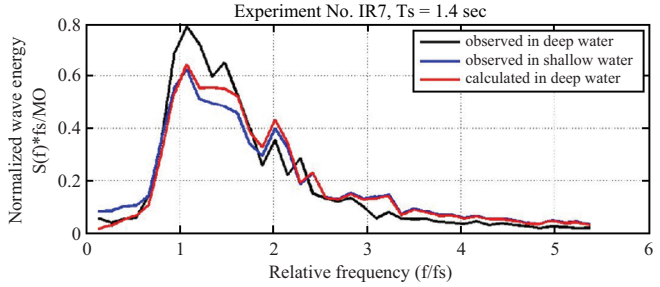

Fig. 13. A comparison of the reverse-calculated wave energy values and the experimental wave energy values (significant wave period Ts = 1.4 sec). f_s is the significant wave period in relation to the corresponding significant frequency.

Eq. (8) to calculate the assigned water depth (0.2 m), is shown in Fig. 6.

(b) The shallow-water spectrum $S(f_i)$ can be obtained using the Fourier transform of the time-series variations in water height at the wave height gauge within the shallow-water region. To analyze variations in the spectral types, the wave energy is normalized, as shown in Eq. (11), to obtain the normalized shallow-water observation wave spectrum $F\left(\frac{f}{f_s}\right)$:

$$\frac{S(f_i)f_s}{m_0} = F\left(\frac{f}{f_s}\right) \tag{11}$$

where f_s is the significant wave period in relation to the corresponding significant frequency and m_0 is the zero-th moment of the spectral density function: $m_0 = \int_0^\infty S(f)df$.

(c) $S'(f_i)$, the calculated value of the deep-water spectrum, is obtained by substituting $K_{spectrum}$, the spectrum transform coefficient, and $S(f_i)$, the shallow-water spectrum, into Eq. (9). After normalization, the normalized, observed deep-water spectrum $F'\left(\frac{f}{f_s}\right)$ is obtained.

(d) Using the Fourier transform of the time-series variations of the water height at the wave height gauge within the deep-water region, the spectrum of the deep-water spectrum $S_o(f_i)$ can be obtained. This spectrum can be normalized to obtain the observed shallow-water wave spectrum $F_o\left(\frac{f}{f_s}\right)$.

(e) Comparisons between the calculated $F'\left(\frac{f}{f_s}\right)$ and observed $F_o\left(\frac{f}{f_s}\right)$, the analysis of the applicability of the reverse linear deduction spectrum, and the corresponding results are shown in Figs. 7-13.

As shown in Fig. 6, in the 0.2 m-deep region, the spectrum transform coefficient varies in relation to the different wave frequencies. This result is due to the fact that the component wavelengths in the high frequency domain are shorter; their propagation toward the near-shore areas will not be significantly affected by the water depth. Therefore, the spectrum transform coefficient is assumed to be 1. When the frequency of the component waves decreases to 2.2 Hz, the topography begins to affect the wave deformations. The wave spectrum transform coefficients increase gradually; at 1.1 Hz, the coefficient increases to 1.2, and at 0.3 Hz, the coefficient decreases to 0.5. Thus, as observed for the irregular waves, the spectrum transform coefficient is more sensitive to irregular waves that have a principal frequency of approximately 1 Hz.

Based on the results shown in Figs. 7-13, the spectra will exhibit significant variations as waves propagate from deep regions to shallow regions. The differences between the two regions become more significant as the wave periods increase. One of the important changes observed is that the wave energy decreases at the wave crests. Therefore, the reverse-calculation method for deep-water spectrum is only reasonable if the peak energy decreases. This study is based on the linear deduction method for waves, and the calculated results (the red line in Figs. 7-13) show that the reverse deep-water wave spectrum falls between the observed shallow water wave spectrum (the blue line in Figs. 7-13) and the observed deep-water wave spectrum (the black line in Figs. 7-13). Importantly, these results are within 0.6-2 times the principal frequency and approach the trends and spectral energy values of the observed deep-water spectrum. Thus, this method apparently modifies the structures of the wave spectra. In subsequent research, the results from this study will be used in the calculation of deep-sea wave data, which will then be used as the data source for differential data assimilation.

IV. CONCLUSIONS

The reverse-calculation method for wave spectra proposed in this paper is able to determine the peak energy values, but the energy of the high-frequency regions is not completely accurate. This error occurs because the derived spectrum transform coefficient is based on first-order linear wave theory, which accounts for the role of linear wave deformation on the energy. This effect is not sensitive to the high-frequency domain, and therefore, the results obtained for the high-frequency components of the deep-water wave energy cannot be effectively adjusted. In this experimental study, the horizontal distance between the shallow- and deep-water regions is 8 m, which corresponds to only 5-6 wavelengths of the peak energy for the low-frequency wave components. During wave propagation, this distance is not suitable for revealing the higher-order non-linear deformations and wave-wave interactions. For the high frequency components, the distance between the shallow- and deep-water regions must reach one or more tens of wavelengths to markedly enhance the higher-order non-linear deformations and wave-wave interactions. This phenomenon appears in the second-order spectrum, which must be solved using non-linear wave theory. The actual wave spectrum in the presence of strong wind, such as the JONSWAP spectrum, is a narrow-band spectral type in which the energy is concentrated in the peak frequency component and the energy of the high-frequency domain is relatively small and can be ignored. Therefore, this method for calculating the reverse spectrum is compatible with actual demands.

ACKNOWLEDGMENTS

The authors would like to thank the Central Weather Bureau and the Water Resources Agency for providing the observed wave data. Thanks are also credited to the Department of Hydraulic & Ocean Engineering in Cheng Kung University for providing the cross-sectional tank with Prof. Chia Chuen Kao's students with a master degree assisting in conducting the experiments. The present study is funded and supported by National Science Council granted as NSC-98-2611-M-211-001.

REFERENCES

1. Chien, C. C. and Kuo, Y. Y., "A study on the spectral form of nearshore water waves," *Proceedings of the 16th Ocean Engineering Conference in Taiwan*, Republic of China, pp. 193-210 (1994). (in Chinese)
2. Goda, Y., *Random Seas and Design of Marine Structures*, University of Tokyo Press (1985).
3. Hasselmann, K., Barnett, T. P., Bouws, E., Carlson, H., Cartwright, D. E., Enke, K., Ewing, J. A., Gienapp, H., Hasselmann, D. E., Kruseman, P., Meerburg, A., Mller, P., Olbers, D. J., Richter, K., Sell, W., and Walden, H., *Measurements of Wind-wave Growth and Swell Decay During the Joint North Sea Wave Project (JONSWAP)*, Ergnzungsheft zur Deutschen Hydrographischen Zeitschrift Reihe, A8, No. 12 (1973).
4. Kuo, Y. Y., Chin, Y. F., and Luo, K. S., "The characteristics of wave spectral from in shallow water," *Proceedings of the 17th Ocean Engineering Conference in Taiwan*, Republic of China, pp. 177-192 (1995). (in Chinese)
5. Ou, S. H., *Parametric Determination of Wave Statistics and Wave Spectrum of Gravity Waves*, Ph. D. Dissertation, National Cheng Kung University, Taiwan, Republic of China (1977).
6. Shuto, N., "Nonlinear long waves in a channel of variable section," *Coastal Engineering in Japan*, Vol. 17, pp. 1-12 (1974).
7. Svendsen, I. A. and Jonsson, I. G., *Hydrodynamics of Coastal Waters*, Technical University of Denmark (1982).
8. Taiwan Power Company, *The Workarounds on Yan-Liao and Fu-Long Coastal Evolution-Wave Investigation of Marine Phenomena Monitoring*, Special Report (2009). (in Chinese)